



Original Article

The Therapeutic Effects of Baicalein on the Hepatopulmonary Syndrome in the Rat Model of Chronic Common Bile Duct Ligation

Ziyang Zeng^{1#}, Yuhao Lei^{1#}, Chunyong Yang¹, Xianfeng Wu¹, Liang Zhang², Zhiyong Yang¹, Lin Chen¹, Xiaobo Wang³, Karine Belguise³, Yujie Li^{1*} and Bin Yi^{1*}

¹Department of Anesthesiology, Southwest Hospital, Third Military Medical University, Chongqing, China; ²Department of Anesthesiology, Chongqing Traditional Chinese Medicine Hospital, Chongqing, China; ³MCD, Center de Biologie Intégrative, Université de Toulouse, CNRS, UPS, Toulouse, France

Received: 18 November 2023 | Revised: 2 February 2024 | Accepted: 21 February 2024 | Published online: 18 March 2024

Abstract

Background and Aims: Hepatopulmonary syndrome (HPS) is characterized by arterial oxygenation defects due to pulmonary vascular dilation in liver disease. To date, liver transplantation remains the only effective treatment for HPS. This study aimed to explore the preventative role of baicalein in HPS development. **Methods:** Sixty male rats were randomly assigned to three groups: sham, common bile duct ligation (CBDL), and baicalein, receiving intraperitoneal injections of baicalein (40 mg·kg⁻¹·d⁻¹, diluted in saline) for 21 days. Survival rate, liver and kidney function, and bile acid metabolism levels were evaluated. Liver and lung angiogenesis and hepatic glycogen staining were assessed, and the expression of relevant proteins was evaluated by immunohistochemistry. **Results:** Baicalein improved survival rates and hypoxemia in rats post-CBDL, reducing angiogenic protein levels and enhancing glucose homeostasis. Compared to the untreated group, baicalein suppressed the expression of vascular endothelial growth factor, placental growth factors, matrix metalloproteinase 9 and C-X-C motif chemokine 2, and it increased the expression of glycemic regulatory proteins, including dipeptidyl peptidase-4, sirtuin 1, peroxisome proliferator-activated receptor gamma co-activator 1α, and 6-phospho-

fructo-2-kinase/fructose-2,6-biphosphatase 3. **Conclusion:** Baicalein significantly improves hepatic function and hypoxia in HPS rats by attenuating pathological angiogenesis in the liver and lungs, showing promise as a treatment for HPS.

Citation of this article: Zeng Z, Lei Y, Yang C, Wu X, Zhang L, Yang Z, *et al.* The Therapeutic Effects of Baicalein on the Hepatopulmonary Syndrome in the Rat Model of Chronic Common Bile Duct Ligation. *J Clin Transl Hepatol* 2024; 12(5):496–504. doi: 10.14218/JCTH.2023.00513.

Introduction

Chronic liver disease (CLD) is responsible for approximately 2 million deaths annually worldwide, with 1 million of these deaths attributed to complications arising from cirrhosis. This contributes to a significant disability burden and an increase in healthcare utilization.¹ Hepatopulmonary syndrome (HPS) manifests in 5% to 30% of adults with liver disease,² significantly impacting the median survival rate of patients with CLD compared to those without HPS: (10.6% vs. 40.8%, *p*<0.05).³ HPS is characterized by a clinical trial of CLD, intrapulmonary vasodilation, and abnormal arterial oxygenation.⁴ Presently, liver transplantation is the only effective treatment for HPS.⁵

In recent years, research has focused on the role of vascular tone, monocyte infiltration, and extra-hepatic angiogenesis in developing HPS.^{6,7} Treatments targeting these mechanisms, such as pentoxifylline, methylene blue, and sorafenib, have been validated in experimental models but have shown limited benefit in clinical settings.^{5,8} Methylene blue, a vasoconstrictor inhibiting the cyclic di-GMP pathway has been explored as a treatment option.⁹ However, its administration has not increased PaO₂ levels in HPS patients.¹⁰ Sorafenib, which targets PLGF, has been reported to effectively reduce pathological pulmonary angiogenesis in HPS experimental models.^{6,11} However, it has shown inefficacy in HPS patients.¹² Pentoxifylline, through the inactivation of protein kinase B (AKT), inhibits pulmonary angiogenesis, but its non-selective nature may restrict clinical use. Insights from translational research in HPS highlight the urgent need

Keywords: Baicalein; Hepatopulmonary syndrome; Common bile duct ligation; Angiogenesis; Glucose metabolism; Liver fibrosis; Glycolysis.

Abbreviations: ALP, alkaline phosphatase; ALT, alanine transaminase; AST, aspartate aminotransferase; CBDL, common bile duct ligation; CLD, chronic liver disease; CXCL2, C-X-C motif chemokine2; DAB, 3,3'-diaminobenzidine staining; DBIL, direct bilirubin; DPP4, dipeptidyl peptidase-4; GGT, gamma-glutamyl transferase; H&E, hematoxylin & eosin; HPS, hepatopulmonary syndrome; IL-6, interleukin-6; iNOS, inducible nitric oxide synthase; MMP9, matrix metalloproteinase 9; MTS, Masson trichrome staining; NO, nitric oxide; PAS, periodic acid Schiff staining; P(A-a)O₂, alveolar-arterial oxygen tension gradient; PFKFB3, fructose-2,6-biphosphatase 3; PGC-1α, PPARγ coactivator-1α; PLGF, placental growth factors; SIRT1, Sirtuin 1; STAT3, transcription-3; TBA, thiobarbituric acid; TBIL, total bilirubin; IBIL, indirect bilirubin; TNF-α, tumor necrosis factor-α; VE-cadherin, vascular endothelial cadherin; VEGF, vascular endothelial growth factor; vWf, von willebrand factor; α-SMA, α-smooth muscle.

#Contributed equally to this work.

*Correspondence to: Bin Yi and Yujie Li, Department of Anesthesiology, Southwest Hospital, Third Military Medical University, No 30. Gaotanyan Main Street, Shapingba District, Chongqing 400038, China. ORCID: <https://orcid.org/0000-0001-5840-2086> (BY), <https://orcid.org/0000-0003-3527-5859> (YL). Tel: +86-23-65463270 (BY), E-mail: yibin1974@163.com (BY); lyj09c@163.com (YL).

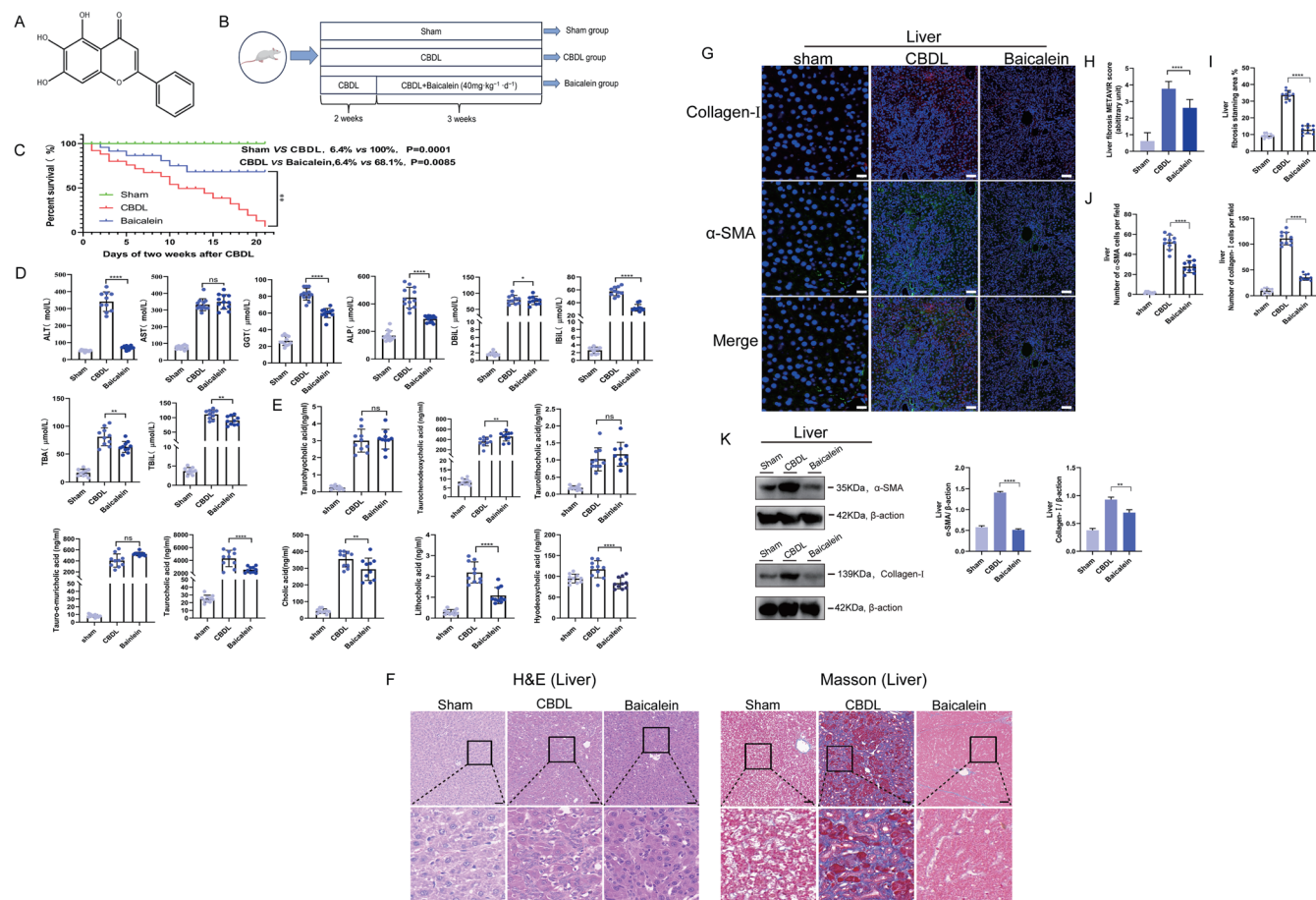


Fig. 1. Effect of baicalein on the liver of the CBDL rats. (A) Molecular structure of baicalein. (B) The detailed diagram of the experimental process. (C) The survival rate of rats in different groups. (D) Liver function and bile acid metabolism test on CBDL rats. Baicalein improved liver enzyme and bilirubin metabolism dysfunction. (E) Baicalein alleviated the level of unconjugated bile acids in the liver. (F, I) HE staining and Masson staining in different groups. Baicalein-reduced liver fibrosis was confirmed by Masson staining. (G, J) Baicalein decreases the expression of collagen-I and α -SMA in CBDL rats. (H) Baicalein improved liver fibrosis METAVIR scores. (K) Western blot analysis of collagen-I and α -SMA levels in different groups (n=3). ns, $p > 0.05$; * $p < 0.05$; ** $p < 0.01$; **** $p < 0.0001$; CBDL, common bile duct ligation.

for treatments that address both liver fibrosis and pulmonary injury while minimizing side effects.^{5,13}

Scutellaria baicalensis Georgi, known for its hepatoprotective properties, has been utilized in traditional Chinese medicine for thousands of years to treat liver diseases. Baicalein (BAL, 5,6,7-trihydroxy-2-phenyl-4H-chromen-4-one), a flavonoid compound derived from the roots of *Scutellaria baicalensis* Georgi (Fig. 1A), offers a broad spectrum of health benefits, including antioxidant, anti-inflammatory, antimicrobial, and hepatoprotective effects.¹⁴ Baicalein accelerates liver recovery post-injury by reducing levels of inflammatory cytokines such as Interleukin-6 (IL-6) and tumor necrosis factor- α (TNF- α) and activating signal transducer and activator of transcription-3 for liver regeneration.^{15,16} Moreover, baicalein has been found to bind directly to Toll-like receptor 4 (TLR4), inhibiting the TLR4/Hypoxia-inducible factors (HIF-1 α)/VEGF signaling pathway,¹⁷ thereby attenuating lung injury by reducing TNF- α production and modulating anti-apoptotic signals.^{18,19} Baicalein also improves glucose metabolism by inhibiting hepatocyte gluconeogenesis via the InsR/IRS-1/PI3K/AKT pathway.²⁰ Notably, high oral doses of baicalein (100–2,800 mg) have been deemed safe and well-tolerated in healthy subjects, suggesting its potential as a viable natural product for clinical applications.²¹ This study

explores baicalein's liver-protecting mechanisms and its therapeutic effect on HPS models induced by CBDL.

Methods

Animal experimentation

Specific-pathogen-free Sprague-Dawley male rats weighing 230 to 330 g were acquired from the Laboratory Animal Center of the Third Military University. The experimental protocols were approved by the Animal Research Committee of the Chongqing Traditional Chinese Medicine Hospital (2021-DWSY-ZZY). The establishment of HPS in rats was achieved through CBDL, as previously described.²² Baicalein, verified by HPLC to be greater than 98% pure (CAS#491-67-8), was sourced from Yuanye Bio-Technology, China, and subsequently diluted in saline. According to Figure 1B, rats were systematically assigned to one of three groups: a sham-operation group (wherein the abdomen was opened and the common bile duct was exposed but not ligated, n=10), a CBDL group (rats were sacrificed five weeks following CBDL, n=30), and a baicalein group (rats received intraperitoneal injections of baicalein at a dose of 40 mg·kg⁻¹·d⁻¹ for three weeks starting two weeks¹⁷ after CBDL, n=20). Prior to the operation, rats underwent an 8-h fast. On the day of sur-

gery, anesthesia was initiated in an isoflurane chamber, with continuous maintenance via isoflurane delivered nasally; 5% isoflurane was used for induction and 2% for maintenance. Post-surgery, rats were positioned laterally on a warming pad set to 37°C. All samples were collected five weeks post-CBDL. The analysis involved three randomly chosen fields from each section of three different rats per group, conducted by two researchers who were blinded to group assignments.

Biochemistry and blood gas analysis

The serum of the rats was collected by puncture into tubes containing anticoagulants and subsequently centrifuged for 10 min at 4,000 rpm at 4°C. This process was carried out to analyze liver biochemistry indicators such as aspartate aminotransferase, alanine transaminase, alkaline phosphatase (ALP), gamma-glutamyl transferase (GGT), total bile acid, total bilirubin, indirect bilirubin (IBIL), and direct bilirubin as evidence of liver injury. These analyses were conducted using an Automatic Biochemistry Analyzer (AU5400, Olympus, Japan). In addition, arterial blood was extracted from the aorta ventralis for arterial blood gas analysis, which was performed using an ABL 700 radiometer (Radiometer Copenhagen, Denmark) in the Clinical Laboratory at Southwest Hospital.

Hematoxylin & Eosin staining, Masson trichrome staining (MTS) and Periodic acid Schiff staining (PAS)

For histological examinations, liver and lung tissues were fixed in 10% formalin for 24 h and then embedded in paraffin. Sections with a thickness of 4 µm were prepared after dehydration in graded ethanol solutions, clearing in chloroform, and embedding in Paraplast. These sections underwent Hematoxylin & Eosin (H&E) staining and PAS staining. Lung injury assessment was based on the H&E stained lung sections according to previously described methods. The degree of liver fibrosis was determined using Masson's trichrome stain, which results in blue staining, and the METAVIR scoring system (F0: No fibrosis, F1: Portal fibrosis without septa, F2: Portal fibrosis with few septa, F3: Numerous septa without cirrhosis, F4: Cirrhosis). Microphotographs of the specimens were captured using a light microscope (Olympus BX51-PMS, Tokyo, Japan), and the images were analyzed with Image-Pro Plus software (version 6.0, Media Cybernetics, Inc., USA).

Immunohistochemical and Immunofluorescence Staining

For *in vivo* 3,3'-diaminobenzidine (DAB) staining, 4-µm-thick paraffin sections were initially dewaxed and subjected to heat-mediated antigen retrieval. To quench endogenous peroxidase activity, sections were treated with 3% H₂O₂ in methanol for 30 min before being incubated with serum. This was followed by incubation with primary antibodies, including rabbit anti-VEGF (1:100, 19003-1-AP, Proteintech), rabbit anti-C-X-C motif chemokine 2 (CXCL2) (1:200, 701126, Thermo Fisher Scientific), rabbit anti-PLGF (1:100, 19666, Abcam), rabbit anti-Sirtuin 1 (SIRT1) (1:500, 189494, Abcam), rabbit anti-MMP9 (1:1,000, 76003, Abcam), rabbit anti-Dipeptidyl Peptidase-4 (DPP4) (1:500, 187048, Abcam), rabbit anti-PGC-1α (1:500, 1918383, Abcam), and rabbit anti-PFKFB3 (1:50, 181861, Abcam), and rabbit anti-SIRT1, (1:500, 189494, Abcam) at 4°C overnight. After PBS washes, the slides were incubated with HRP-labeled Goat Anti-Rabbit IgG (H+L) secondary antibodies. The staining patterns of these antibodies were visualized using DAB staining, with hematoxylin used for nuclear counterstaining

and sealed with neutral resin. Ten representative regions per section were randomly selected by an assessor blinded to the treatment groups for analysis. Values were expressed as percentages, comparing the mean value for the sham group to the percentage of positive cells.

For *in vivo* fluorescence staining, 4-µm-thick frozen sections were incubated overnight at 4°C with a range of antibodies: anti-CD31 rabbit antibody (1:400, GB11063-2, Servicebio), anti-inducible nitric oxide synthase (iNOS) rabbit antibody (1:500, GB11119, Servicebio), anti-vascular endothelial cadherin (VE-cadherin) (1:1,000, 205336, Abcam), von Willebrand factor (vWF) (1:200, 6994, Abcam), anti-Collagen-I Rabbit (1:800, GB114197, Servicebio), and anti-α-smooth muscle actin (α-SMA) rabbit antibody (1:500, GB111364, Servicebio). This comprehensive antibody panel targets a variety of cellular markers indicative of angiogenesis, inflammation, and tissue remodeling, essential for understanding the pathological changes within the liver and lung tissues in the context of HPS research.

After washing with PBS, the slides were incubated with fluorochrome-conjugated secondary antibodies, specifically HRP-labeled Goat Anti-Rabbit IgG (H+L), to enhance fluorescence visualization of the antibody staining patterns. The sections were further counterstained with Cy3-labeled Goat Anti-Rabbit IgG (H+L) and FITC-labeled Goat Anti-Rabbit IgG (H+L), providing a multicolor immunofluorescence landscape. Nuclei were stained with DAPI (4,6-diamidino-2-phenylindole), offering a sharp contrast with its characteristic blue fluorescence. The sections were examined using an Imager.A2 microscope (ZEISS, Germany). Immunofluorescence quantification was performed utilizing ImageJ software (National Institutes of Health). Five fields were randomly selected for analysis using Panoramic MIDI (3DHISTECH, Hungary) for each immunofluorescence-labeled section. The enumeration of CD31-positive cells per high-power field was facilitated by Image-Pro Plus software (version 6.0, Media Cybernetics Inc, USA), ensuring precise quantitative assessment.

Western blotting analysis

Briefly, total proteins were extracted from 60 mg of liver and lung tissues using a total protein extraction kit suitable for animal-cultured cells and tissues (Epizyme Biotech, PC201, China). The concentration of the extracted proteins was determined by the BCA method (Thermo, SF247582, USA). These denatured proteins were then separated on 7.5% SDS-PAGE (Epizyme Biotech, PG211, China) and transferred onto polyvinylidene fluoride membranes for subsequent analysis. After blocking non-specific binding sites with BSA, the membranes were incubated overnight at 4°C with primary antibodies targeted against α-SMA (1:1,000, ab7817, Abcam), collagen-I (1:1,000, bs-10423R, Bioss), vWF (1:1,000, ab6994, Abcam), VE-cadherin (1:1,000, ab231227, Abcam), iNOS (1:1,000, 22226-1-AP, Proteintech), PGC1 (ab191838, Abcam), and PFKFB3 (ab181861, Abcam). Following incubation, the membranes were washed with TBST containing 0.1% Tween-20 and incubated with an HRP-conjugated secondary antibody goat anti-rabbit (Beyotime, A0208, Biotechnology, China) at a 1:1,000 dilution for 1 h at room temperature. After three washes with TBST, the immunoreactive bands were visualized using an ECL chemiluminescent kit (Thermo, XF345252, USA), providing a robust method for protein expression analysis.

Enzyme-linked immunosorbent assay (ELISA)

To prepare liver tissue samples, 0.06 g of liver tissue was homogenized in 1 ml of PBS using a Bead Ruptor 24 (OMNI,

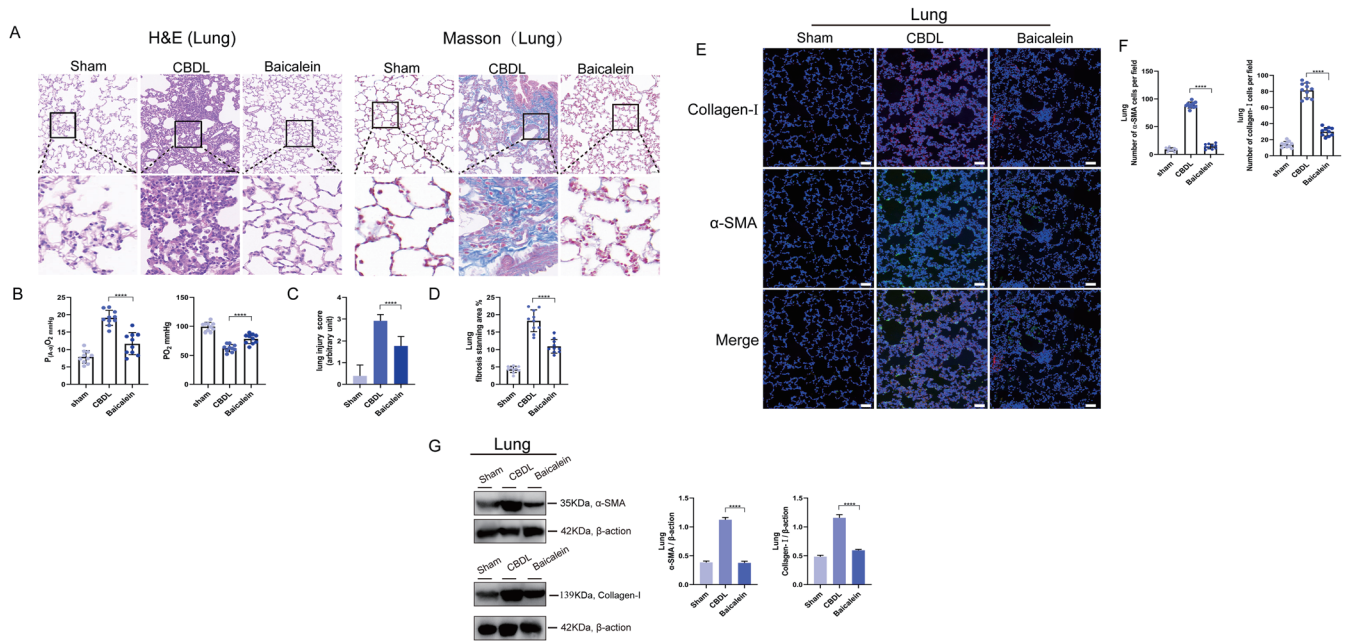


Fig. 2. Effects of baicalein on the lung of CBDL rats. H&E (A) and MTS confirmed that baicalein significantly reduced lung inflammatory infiltration and fibrosis in CBDL rats. (B) The effect of baicalein on hypoxemia in CBDL rats. (C) The lung injury score showed a lower score and fewer injuries in the baicalein group. (D) Baicalein alleviates pulmonary fibrosis in baicalein groups by MTS. (E, F) Representative images of Collagen-I (red) and α -SMA (green) immunostaining. (G) Western blot analysis of collagen-I and α -SMA levels in different groups (n=3). Nuclei, DAPI (blue). Scale bar, 50 μ m; **** p <0.0001; CBDL, common bile duct ligation; H&E, hematoxylin & eosin; MTS, masson trichrome staining.

USA). The homogenate was centrifuged at 12,000 rpm and 4°C for 15 min, and the supernatant was collected for subsequent analysis. The levels of glycogen phosphorylase (GPase) and glycogen synthase (GS) were determined using ELISA kits (JT-T1106 and JT-T1104, Jianglaibio, China). Similarly, MMP9 and CXCL2 levels were measured using ELISA (EK1463 and EK0725, Boster Biological Technology, China), and VEGF and PLGF levels were assessed with ELISA kits (RA20124 and RA20510, Bioswamp, China). Samples and the reagent solution were added to a 96-well plate and incubated according to the kit instructions for 10 min and 5 min, respectively. Absorbance levels A1 and A2 were read at 340 nm and 450 nm, respectively. The difference in $A=A_2-A_1$ was used to calculate GPase (nmol/min/g)= $238.7*(\Delta A+0.0173)/0.05$ g; GS (nmol/min/g)= $160.8*\Delta A/0.05$ g.

Statistical analysis

All measurements were presented as means \pm SD. The data were analyzed using students’ *t*-tests or ANOVA with Bonferroni correction for multiple group comparisons using GraphPad Prism 7.0 software (Inc., La Jolla, CA, USA). A *p*-value<0.05 was considered statistically significant. *p*<0.05 was considered statistical significance.

Results

Baicalein improved the liver function and outcome of the CBDL rats

We evaluated the therapeutic effect of baicalein on the liver function and survival outcome of rats subjected to common bile duct ligation (CBDL). Notably, baicalein significantly improved the survival rate of CBDL rats (CBDL vs. Baicalein: 6.4% vs. 68.1%, *p*=0.0085). Furthermore, baicalein administration resulted in a noticeable decrease in serum GGT, ALP,

and IBiL levels, which had initially increased following CBDL (GGT: 82.67 μ mol/L vs. 60 μ mol/L, *p*<0.0001; ALP: 445.9 μ mol/L vs. 290.6 μ mol/L, *p*<0.0001; IBiL: 57.5 μ mol/L vs. 32.4 μ mol/L, *p*<0.0001). Baicalein also enhanced bile acid metabolism, indicated by reduced levels of unconjugated bile acids such as taurocholic acid and hyodeoxycholic acid (Fig. 1D, E).

Histological analysis via HE and Masson staining revealed that baicalein mitigated liver fibrosis in CBDL rats, evidenced by decreased inflammatory cell infiltration, improved liver fibrosis scores, and reduced fibrosis deposition. Compared to the CBDL group, the baicalein group exhibited significantly reversed pathological tissue structures and improved liver fibrosis METAVIR scores (Fig. 1F, H, I). Significant fibrosis progression was observed in the CBDL group compared to the sham group, but baicalein treatment decreased the expression of collagen-I and α -SMA (Fig. 1G, J). We observed that collagen-I and α -SMA have significantly higher expression levels than collagen-I and α -SMA in baicalein groups (Fig. 1K).

Baicalein improved the hypoxemia of the CBDL rats

The study investigated the effects of baicalein on lung inflammation and fibrosis in CBDL rats. Baicalein showed a significant reduction in lung inflammatory response and fibrosis, as evidenced by HE and Masson staining tests (Fig. 2A). It notably improved alveolar gas exchange, indicated by decreased alveolar-arterial oxygen gradient ($P_{(A-a)}O_2$) and increased arterial oxygen partial pressure (PO_2) in CBDL rats ($P_{(A-a)}O_2$: Sham vs. CBDL vs. Baicalein - 7.38 mmHg vs. 19.12 mmHg vs. 11.8 mmHg, *p*<0.0001; PO_2 : Sham vs. CBDL vs. Baicalein - 98.82 mmHg vs. 62.68 mmHg vs. 80.42 mmHg, *p*<0.0001) (Fig. 2B). Additionally, baicalein was found to improve lung injury scores (Fig 2C), reverse fibrosis progression (Fig. 2D), and reduce the expression of fibrotic markers, collagen-I and α -SMA, in the lung tissues of

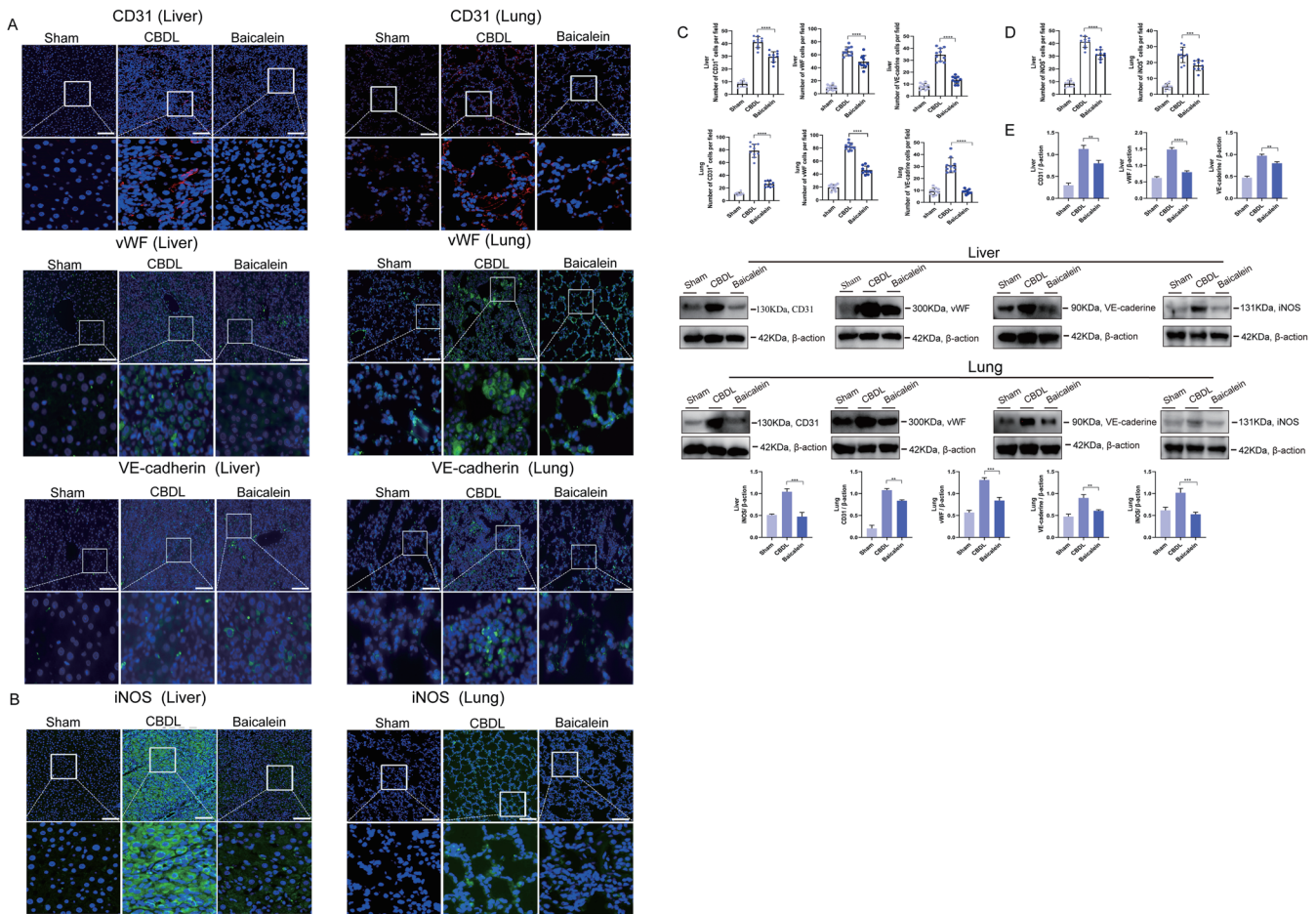


Fig. 3. Effects of baicalein on the pathological angiogenesis of the liver and lung in the CBDL rats and the expression of vasodilation-related proteins. (A, C) The numbers of CD31 (red), vWF (green) and VE-cadherin (green) cells in different groups by immunofluorescence staining. (B, D) The numbers of iNOS (green) expression in different groups by immunofluorescence staining. (E) Western blot analysis of CD31 (red), vWF, VE-cadherin, and iNOS levels in different groups and baicalein alleviate the expression of CD31 (red), vWF, VE-cadherin, and iNOS (n=3). Nuclei, DAPI (blue). ***p*<0.01; ****p*<0.001; *****p*<0.0001. Scale bar, 50 μm; CBDL, common bile duct ligation; vWF, von willebrand factor; VE-cadherin, vascular endothelial cadherin; iNOS, inducible nitric oxide synthase.

CBDL rats (Fig. 2E-F). These findings suggest that baicalein enhances lung function, reduces inflammatory cell infiltration, and restores normal alveolar tissue structure, with reduced collagen-I staining confirmed by Masson staining. We observed that collagen-I and α-SMA have significantly higher lung expression levels than collagen-I and α-SMA in baicalein groups (Fig 2G).

Baicalein reduces the pathological angiogenesis of the liver and lung in CBDL rats

We analyzed angiogenesis endothelial markers CD31, vWF, and VE-cadherin and found extensive angiogenesis in the liver and lung of CBDL rats. Compared with the sham group, CD31, vWF, and VE-cadherin expression levels were significantly enhanced in the CBDL group. Baicalein reduced the expression of CD31, vWF, and VE-cadherin in lung tissue and the liver (Fig. 3A, C). We further assessed the expression of angiogenesis-associated proteins. Baicalein decreased iNOS expression and demonstrated a reduced pathological vasodilatory state (Fig. 3B, D). We observed that CD31, vWF, VE-cadherin, and iNOS have significantly higher expression levels in CBDL, and baicalein mitigated the expression of CD31, vWF, VE-cadherin, and iNOS (Fig. 3E).

Baicalein reduces the expression of angiogenesis-associated proteins in CBDL rats

Accompanying the reduction in pathological angiogenesis within the liver and lungs of rats treated with baicalein, a decrease in angiogenesis-associated proteins was observed via immunohistochemistry (Fig. 4A, B). Specifically, the expression levels of angiogenesis-related proteins such as VEGF, PLGF, MMP9, and CXCL2 were significantly elevated in the CBDL group compared to the sham group. Baicalein treatment resulted in a reduction of VEGF, PLGF, MMP9, and CXCL2 expression levels and inhibited the release of these angiogenesis proteins when compared to the CBDL group. We evaluated the expression of VEGF, PLGF, MMP9, and CXCL2 levels in different groups. A comparison of CBDL vs. baicalein showed decreased VEGF, PLGF, MMP9, and CXCL2 levels, indicating that baicalein alleviated angiogenesis (Fig. 4C).

Effect of baicalein on liver glycogen and glucose metabolism associated proteins in CBDL rats

Liver cirrhosis is often accompanied by abnormal glucose metabolism, which may exacerbate the condition. An abnormal accumulation of liver glycogen was observed in CBDL

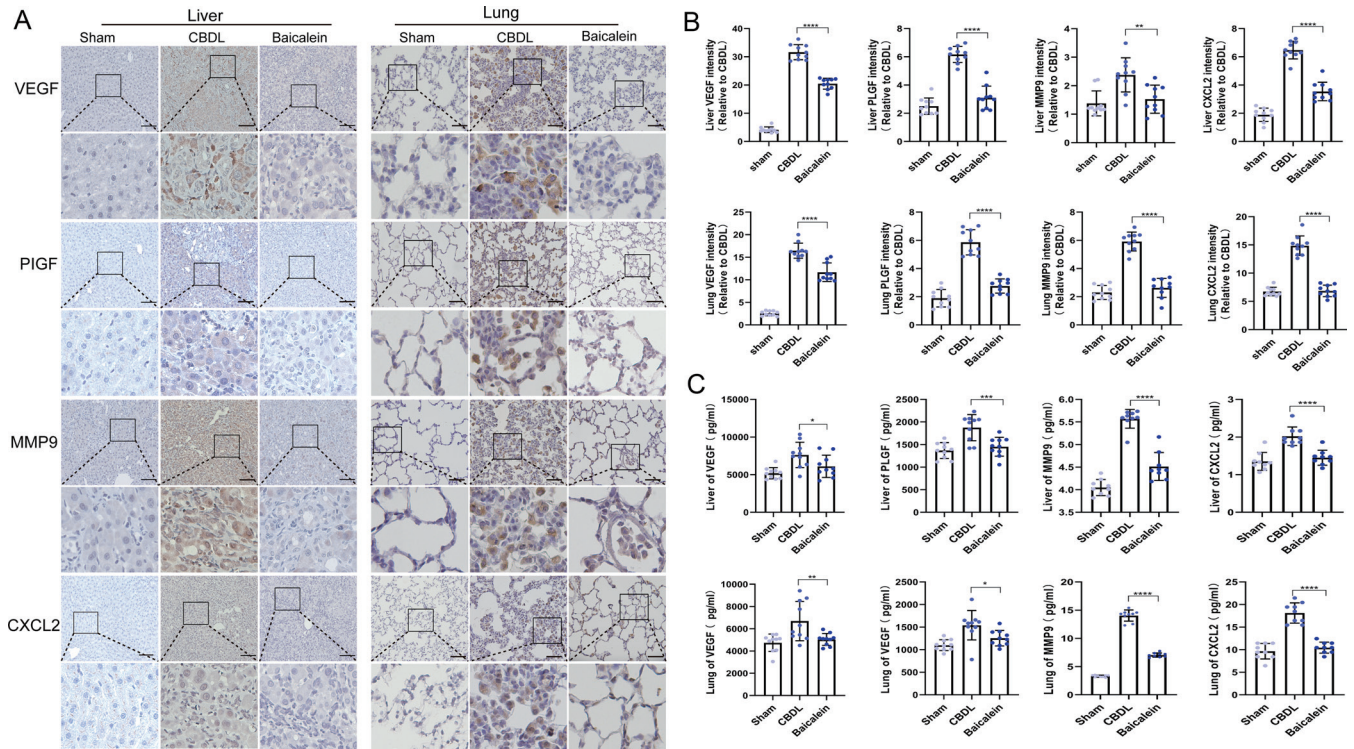


Fig. 4. Baicalein attenuates the expression of angiogenesis-related proteins. (A-B) The expression of (A, B) VEGF, PLGF, and pro-angiogenic factors MMP-9 and CXCL2 in the liver and lung of rats in sham, CBDL, and baicalein groups. (C) Evaluation of VEGF, PLGF, MMP9, and CXCL2 levels in different groups indicated baicalein alleviated angiogenesis. * $p < 0.05$; ** $p < 0.01$; *** $p < 0.001$; **** $p < 0.0001$; Scale bar, 50 μm ; VEGF, vascular endothelial growth factor; PLGF, Placental growth factors; MMP9, matrix metalloproteinase 9; CXCL2, C-X-C motif chemokine 2.

rats using PAS staining, while baicalein treatment significantly improved glycogen accumulation in liver tissue (Fig. 5A, B). Baicalein was found to enhance the activity of glycogen-metabolizing enzymes, improve glycogen storage in liver tissue, and promote glycogen utilization (Fig. 5C). Changes in the expression of proteins associated with cellular glucose metabolism were also assessed by immunohistochemistry. Baicalein limited the expression levels of DPP4 and PFKFB3 while promoting the expression of SIRT1 and PGC-1 α , thereby alleviating liver fibrosis (Fig. 5D, E). Examination of PGC-1 α and PFKFB3 levels showed that baicalein enhanced PGC-1 α and mitigated PFKFB3 expression, effectively reversing the levels of these proteins to normal (Fig. 5F, G).

Discussion

In this study, we discovered that baicalein mitigates liver fibrosis and improves hypoxemia, potentially through the regulation of glucose metabolism to reduce pathological angiogenesis in both the liver and lungs. Pathological angiogenesis has recently been recognized as a vital mechanism underlying HPS.^{11,23} However, the first RCT focused on anti-angiogenic therapy did not significantly improve hypoxemia and negatively impacted the quality of life.¹² Interestingly, HPS almost invariably resolves following liver transplantation, highlighting that alleviating liver injury should be a primary treatment goal for HPS.

Baicalein, metabolized from baicalin by gut microbiota, is derived from traditional Chinese herbal medicine^{18,20} and has been shown in previous studies to inhibit the expression levels of pro-inflammatory cytokines such as TNF- α and IL-6.^{24,25} Furthermore, it reduces the expression of pro-an-

giogenic and angiogenesis-related proteins, including VEGF and PLGF.^{6,11,14} It inhibits the activity of MMP9, which plays a crucial role in the degradation of the extracellular matrix, a critical step in angiogenesis.¹⁴ Our findings corroborate these earlier reports, showing that baicalein significantly reduces the expression of VEGF and PLGF. Additionally, baicalein treatment decreased the levels of CXCL2 and MMP9 in the liver and lungs of CBDL groups, addressing pathological angiogenesis and its associated fibrosis.²⁶

These results suggest that baicalein, through its multifaceted biological activities, offers a promising therapeutic approach to treating HPS by targeting the inflammatory and fibrotic pathways and the angiogenic mechanisms contributing to the disease's pathophysiology.

The recent understanding that glucose metabolism levels are intricately linked with fibrosis highlights the complex interplay between metabolic pathways and liver disease progression.^{27,28} DPP4 has been identified as a surface protein enriched in vascular endothelial cells²⁹ and has been associated with liver disease severity and fibrosis.³⁰ Elevated plasma concentrations of DPP4 correlate with the severity of liver disease, whereas a decrease in DPP4 levels contributes to glucose homeostasis by reducing hepatic gluconeogenesis.³¹ This regulatory mechanism suggests that targeting DPP4 could offer therapeutic benefits in managing liver disease and associated metabolic dysfunctions.

SIRT1 operates as a nicotinamide adenine dinucleotide-dependent deacetylase involved in various metabolic processes, including glucose metabolism and mitochondrial biogenesis. The activation of SIRT1 enhances insulin sensitivity and glucose homeostasis, and it plays a critical role in mitigating fibrosis by promoting the renewal of hepatic

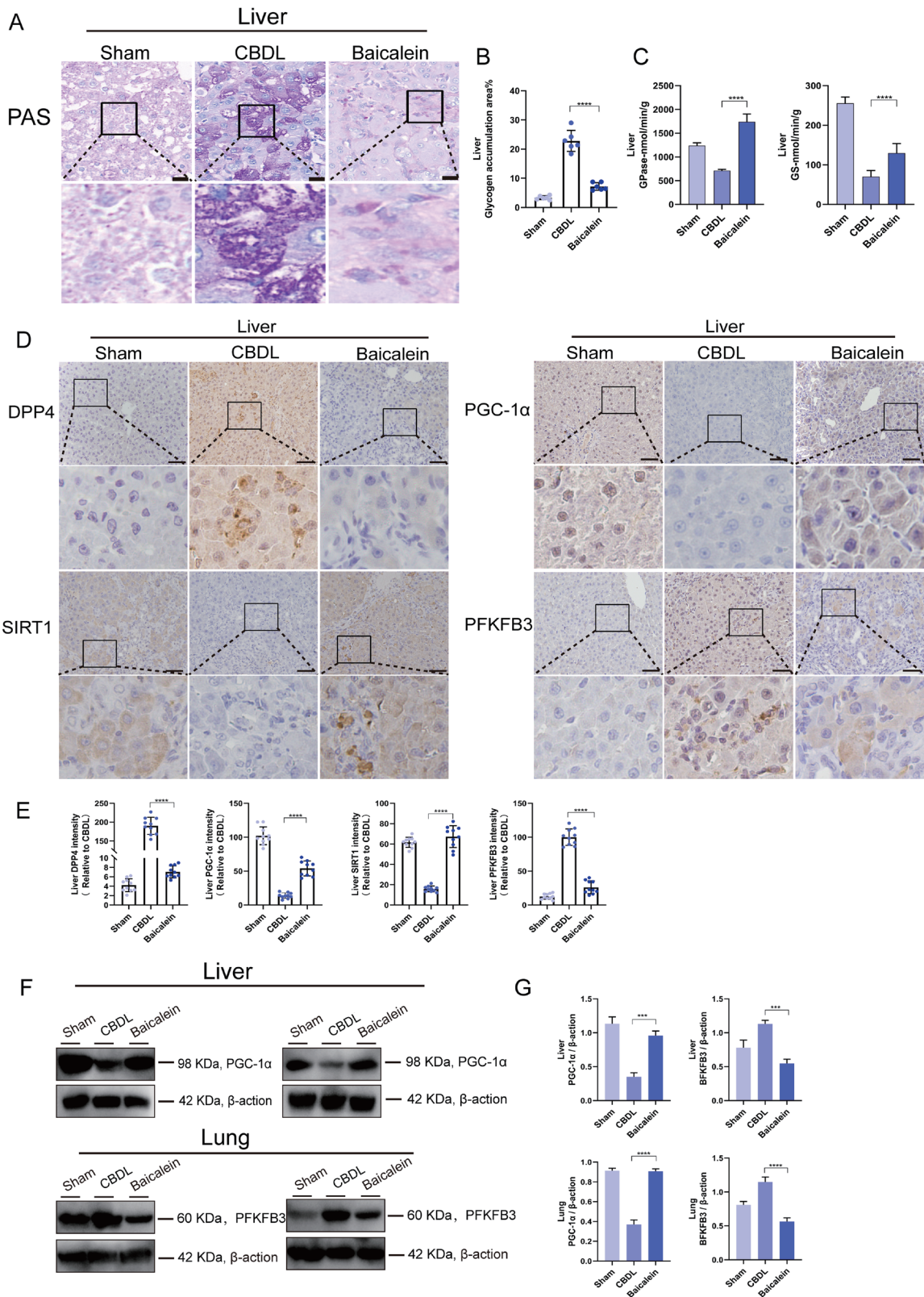


Fig. 5. The effect of baicalein on glucose metabolism in the liver. (A, B) Baicalein increases the content of glycogen in liver tissue. Scale bar, 20 μ m. (C) The effect of baicalein on the activity of glycogen-metabolizing enzymes. (D, E) The effect of baicalein on glucose metabolism-related proteins. (F, G) Western blot analysis of PGC-1 α and PFKFB3 levels in different groups. Scale bar, 50 μ m; *** p <0.001; **** p <0.0001; PGC-1 α , PPAR γ coactivator-1 α ; PFKFB3, fructose-2,6-bisphosphatase 3.

astrocytes.³² DPP4 inhibition has been shown to depend on the activation of SIRT1,^{33–35} linking these two proteins in a regulatory axis that controls blood glucose levels in conditions like CBDL-induced liver damage and slows the progression of fibrosis in hepatic astrocytes.

PGC-1 α is recognized as a transcriptional co-activator that enhances the function of numerous transcription factors involved in mitochondrial biogenesis and glucose metabolism.³⁶ PFKFB3, a protein involved in glycolysis, contributes to the metabolic adjustments required under fibrotic conditions and vessel sprouting. The knockdown of PFKFB3 leads to reduced glycolytic flux and suppresses the hypermetabolic state induced by fibrosis.^{37,38} PGC-1 α has been shown to negatively regulate PFKFB3, suggesting that the activation of PGC-1 α signaling can ameliorate fibrosis by downregulating PFKFB3, thereby reducing glycolysis flux.³⁹ This intricate network of metabolic regulators—DPP4, SIRT1, PGC-1 α , and PFKFB3 offers potential therapeutic targets for addressing the metabolic alterations associated with liver fibrosis. Modulating these pathways may improve glucose metabolism, reduce hepatic gluconeogenesis, and slow fibrosis progression, offering a multifaceted approach to treating liver diseases.

Compared with the CBDL group, baicalein modulates homeostasis by inhibiting the expression of DPP4 and PFKFB3 while enhancing SIRT1 and PGC-1 α levels to improve tissue fibrosis and maintain glucose metabolism. Fibrosis necessitates substantial energy consumption.^{37,40} The depletion of glycogen in the CBDL model has been substantiated by PAS staining; baicalein partially restores glycogen content in the liver through glucose metabolism regulation. Moreover, baicalein mitigates energy consumption by modulating glucose metabolism, thereby ameliorating liver fibrosis.

This study acknowledges certain limitations. Primarily, the baicalein intervention commenced 14 days post-CBDL model establishment, with specimen analysis following three weeks of continuous treatment. Although this timeframe aligns with standard observation periods for CBDL rat interventions, extended studies are warranted to evaluate baicalein's long-term impacts. Secondly, due to baicalein's poor water solubility and intestinal absorption, intraperitoneal injection was employed to enhance absorption, a method not typically utilized in clinical settings. This necessitates further research to identify the most effective administration route. Lastly, baicalein's clinical use often involves combination with other decoctions, necessitating additional studies to understand potential drug interactions.

In conclusion, baicalein significantly attenuates pulmonary angiogenesis by suppressing VEGF, PLGF, CXCL2, and MMP9 expression. It also alleviates liver fibrosis by activating the glucose metabolism signaling pathway, improving hypoxemia in CBDL rats. Our findings suggest baicalein as a promising therapeutic strategy for treating HPS.

Acknowledgments

The authors pay tribute to all the care and support that has gone into the research. We thank Medjaden Inc. for scientific editing of this manuscript.

Funding

The work was supported by the National Science Foundation of China (No. 82070630 to BY, No. 82100658 to YL), Science Foundation of Chongqing (cstc2019jcyj-msxmX0667 to ZZ), and National Key R&D Program of China (No. 2018YFC0116702 to BY).

Conflict of interest

The authors have no conflict of interest related to this publication.

Author contributions

Study concept and design (ZZ, BY, YjL), acquisition of data (YhL, ZY), analysis and interpretation of data (ZY, CY), drafting of the manuscript (ZZ, YhL), critical revision of the manuscript for important intellectual content (KB, LZ), administrative, technical, or material support (LC, XfW), and study supervision (BY, XbW, YjL). All authors have contributed significantly to this study and approved the final manuscript.

Ethical statement

All experimental procedures were approved by the Animal Research Committee of Chongqing Traditional Chinese Medicine Hospital (2021-DWSY-ZZY).

Data sharing statement

Some or all data, models, or codes generated or used during the study are available from the corresponding author upon request.

References

- [1] Asrani SK, Devarbhavi H, Eaton J, Kamath PS. Burden of liver diseases in the world. *J Hepatol* 2019;70(1):151–171. doi:10.1016/j.jhep.2018.09.014, PMID:30266282.
- [2] Rodríguez-Roisin R, Krowka MJ. Hepatopulmonary syndrome—a liver-induced lung vascular disorder. *N Engl J Med* 2008;358(22):2378–2387. doi:10.1056/NEJMra0707185, PMID:18509123.
- [3] Soulaïdopoulos S, Cholongitas E, Giannakoulas G, Vlachou M, Goulis I. Review article: Update on current and emergent data on hepatopulmonary syndrome. *World J Gastroenterol* 2018;24(12):1285–1298. doi:10.3748/wjg.v24.i12.1285, PMID:29599604.
- [4] Palma DT, Fallon MB. The hepatopulmonary syndrome. *J Hepatol* 2006;45(4):617–625. doi:10.1016/j.jhep.2006.07.002, PMID:16899322.
- [5] Del Valle K, DuBrock HM. Hepatopulmonary Syndrome and Portopulmonary Hypertension: Pulmonary Vascular Complications of Liver Disease. *Compr Physiol* 2021;11(4):3281–3302. doi:10.1002/cphy.c210009, PMID:34636408.
- [6] Raevens S, Fallon MB. Potential Clinical Targets in Hepatopulmonary Syndrome: Lessons From Experimental Models. *Hepatology* 2018;68(5):2016–2028. doi:10.1002/hep.30079, PMID:29729196.
- [7] Wang D, Yang C, Zeng Z, Wu X, Liang H, Hu X, *et al*. Extrahepatic Angiogenesis: A Potential Common Pathophysiological Basis of Multiple Organ Dysfunction in Rats with Cholestasis Cirrhosis. *Front Biosci (Landmark Ed)* 2023;28(10):272. doi:10.31083/j.fbl2810272, PMID:37919052.
- [8] Zhang J, Fallon MB. Hepatopulmonary syndrome: update on pathogenesis and clinical features. *Nat Rev Gastroenterol Hepatol* 2012;9(9):539–549. doi:10.1038/nrgastro.2012.123, PMID:22751459.
- [9] Miyamoto A, Katsuta Y, Zhang XJ, Li HL, Ohsuga M, Komeichi H, *et al*. Effect of chronic methylene blue administration on hypoxemia in rats with common bile duct ligation. *Hepatol Res* 2010;40(6):622–632. doi:10.1111/j.1872-034X.2010.00640.x, PMID:20412326.
- [10] Gupta S, Tang R, Al-Hesayen A. Inhaled nitric oxide improves the hepatopulmonary syndrome: a physiologic analysis. *Thorax* 2021;76(11):1142–1145. doi:10.1136/thoraxjnl-2020-216128, PMID:33859047.
- [11] Chang CC, Chuang CL, Lee FY, Wang SS, Lin HC, Huang HC, *et al*. Sorafenib treatment improves hepatopulmonary syndrome in rats with biliary cirrhosis. *Clin Sci (Lond)* 2013;124(7):457–466. doi:10.1042/CS20120052, PMID:23043394.
- [12] Kawut SM, Ellenberg SS, Krowka MJ, Goldberg D, Vargas H, Koch D, *et al*. Sorafenib in Hepatopulmonary Syndrome: A Randomized, Double-Blind, Placebo-Controlled Trial. *Liver Transpl* 2019;25(8):1155–1164. doi:10.1002/lt.25438, PMID:30816637.
- [13] Tugues S, Fernandez-Varo G, Muñoz-Luque J, Ros J, Arroyo V, Rodés J, *et al*. Antiangiogenic treatment with sunitinib ameliorates inflammatory infiltrate, fibrosis, and portal pressure in cirrhotic rats. *Hepatology* 2007;46(6):1919–1926. doi:10.1002/hep.21921, PMID:17935226.
- [14] Dinda B, Dinda S, DasSharma S, Banik R, Chakraborty A, Dinda M. Therapeutic potentials of baicalin and its aglycone, baicalein against inflammatory disorders. *Eur J Med Chem* 2017;131:68–80. doi:10.1016/j.ejmech.2017.03.004, PMID:28288320.
- [15] Madrigal-Santillán E, Madrigal-Bujaidar E, Álvarez-González I, Sumaya-Martínez MT, Gutiérrez-Salinas J, Bautista M, *et al*. Review of natural products with hepatoprotective effects. *World J Gastroenterol* 2014;20(40):14787–

14804. doi:10.3748/wjg.v20.i40.14787, PMID:25356040.
- [16] Huang HL, Wang YJ, Zhang QY, Liu B, Wang FY, Li JJ, *et al*. Hepatoprotective effects of baicalein against CCl₄-induced acute liver injury in mice. *World J Gastroenterol* 2012;18(45):6605–6613. doi:10.3748/wjg.v18.i45.6605, PMID:23236235.
- [17] Li P, Zhang R, Wang M, Chen Y, Chen Z, Ke X, *et al*. Baicalein Prevents Fructose-Induced Hepatic Steatosis in Rats: In the Regulation of Fatty Acid De Novo Synthesis, Fatty Acid Elongation and Fatty Acid Oxidation. *Front Pharmacol* 2022;13:917329. doi:10.3389/fphar.2022.917329, PMID:35847050.
- [18] Chen Y, Zhang J, Zhang M, Song Y, Zhang Y, Fan S, *et al*. Baicalein resensitizes tamoxifen-resistant breast cancer cells by reducing aerobic glycolysis and reversing mitochondrial dysfunction via inhibition of hypoxia-inducible factor-1 α . *Clin Transl Med* 2021;11(11):e577. doi:10.1002/ctm2.577, PMID:34841716.
- [19] Jiang C, Zhang J, Xie H, Guan H, Li R, Chen C, *et al*. Baicalein suppresses lipopolysaccharide-induced acute lung injury by regulating Drp1-dependent mitochondrial fission of macrophages. *Biomed Pharmacother* 2022;145:112408. doi:10.1016/j.biopha.2021.112408, PMID:34801855.
- [20] Yang Z, Huang W, Zhang J, Xie M, Wang X. Baicalein improves glucose metabolism in insulin resistant HepG2 cells. *Eur J Pharmacol* 2019;854:187–193. doi:10.1016/j.ejphar.2019.04.005, PMID:30970232.
- [21] Lu X, Wu K, Jiang S, Li Y, Wang Y, Li H, *et al*. Therapeutic mechanism of baicalein in peritoneal dialysis-associated peritoneal fibrosis based on network pharmacology and experimental validation. *Front Pharmacol* 2023;14:1153503. doi:10.3389/fphar.2023.1153503, PMID:37266145.
- [22] Liu C, Gao J, Chen B, Chen L, Belguise K, Yu W, *et al*. Cyclooxygenase-2 promotes pulmonary intravascular macrophage accumulation by exacerbating BMP signaling in rat experimental hepatopulmonary syndrome. *Biochem Pharmacol* 2017;138:205–215. doi:10.1016/j.bcp.2017.06.117, PMID:28642034.
- [23] Li YJ, Wu XF, Wang DD, Li P, Liang H, Hu XY, *et al*. Serum Soluble Vascular Endothelial Growth Factor Receptor 1 as a Potential Biomarker of Hepatopulmonary Syndrome. *J Clin Transl Hepatol* 2023;11(5):1150–1160. doi:10.14218/JCTH.2022.00421, PMID:37577229.
- [24] Yang JY, Li M, Zhang CL, Liu D. Pharmacological properties of baicalin on liver diseases: a narrative review. *Pharmacol Rep* 2021;73(5):1230–1239. doi:10.1007/s43440-021-00227-1, PMID:33595821.
- [25] Ganguly R, Gupta A, Pandey AK. Role of baicalin as a potential therapeutic agent in hepatobiliary and gastrointestinal disorders: A review. *World J Gastroenterol* 2022;28(26):3047–3062. doi:10.3748/wjg.v28.i26.3047, PMID:36051349.
- [26] Natsume M, Shimura T, Iwasaki H, Okuda Y, Hayashi K, Takahashi S, *et al*. Omental adipocytes promote peritoneal metastasis of gastric cancer through the CXCL2-VEGFA axis. *Br J Cancer* 2020;123(3):459–470. doi:10.1038/s41416-020-0898-3, PMID:32439934.
- [27] Ryan JJ, Archer SL. The right ventricle in pulmonary arterial hypertension: disorders of metabolism, angiogenesis and adrenergic signaling in right ventricular failure. *Circ Res* 2014;115(1):176–188. doi:10.1161/CIRCRESAHA.113.301129, PMID:24951766.
- [28] Gilgenkrantz H, Mallat A, Moreau R, Lotersztajn S. Targeting cell-intrinsic metabolism for antifibrotic therapy. *J Hepatol* 2021;74(6):1442–1454. doi:10.1016/j.jhep.2021.02.012, PMID:33631228.
- [29] Kim KM, Noh JH, Bodogai M, Martindale JL, Yang X, Indig FE, *et al*. Identification of senescent cell surface targetable protein DPP4. *Genes Dev* 2017;31(15):1529–1534. doi:10.1101/gad.302570.117, PMID:28877934.
- [30] Barchetta I, Ceccarelli V, Cimini FA, Barone E, Sentinelli F, Coluzzi M, *et al*. Circulating dipeptidyl peptidase-4 is independently associated with the presence and severity of NAFLD/NASH in individuals with and without obesity and metabolic disease. *J Endocrinol Invest* 2021;44(5):979–988. doi:10.1007/s40618-020-01392-5, PMID:32852705.
- [31] Muscelli E, Casolaro A, Gastaldelli A, Mari A, Seghier G, Astiarraga B, *et al*. Mechanisms for the antihyperglycemic effect of sitagliptin in patients with type 2 diabetes. *J Clin Endocrinol Metab* 2012;97(8):2818–2826. doi:10.1210/jc.2012-1205, PMID:22685234.
- [32] Yan X, Zhang Y, Peng Y, Li X. The water extract of Radix scutellariae, its total flavonoids and baicalin inhibited CYP7A1 expression, improved bile acid, and glycolipid metabolism in T2DM mice. *J Ethnopharmacol* 2022;293:115238. doi:10.1016/j.jep.2022.115238, PMID:35351576.
- [33] Baci D, Bruno A, Cascini C, Gallazzi M, Mortara L, Sessa F, *et al*. Acetyl-L-Carnitine downregulates invasion (CXCR4/CXCL12, MMP-9) and angiogenesis (VEGF, CXCL8) pathways in prostate cancer cells: rationale for prevention and interception strategies. *J Exp Clin Cancer Res* 2019;38(1):464. doi:10.1186/s13046-019-1461-z, PMID:31718684.
- [34] Chen Z, Yu J, Fu M, Dong R, Yang Y, Luo J, *et al*. Dipeptidyl peptidase-4 inhibition improves endothelial senescence by activating AMPK/SIRT1/Nrf2 signaling pathway. *Biochem Pharmacol* 2020;177:113951. doi:10.1016/j.bcp.2020.113951, PMID:32251672.
- [35] Soare A, Györfi HA, Matei AE, Dees C, Rauber S, Wohlfahrt T, *et al*. Dipeptidylpeptidase 4 as a Marker of Activated Fibroblasts and a Potential Target for the Treatment of Fibrosis in Systemic Sclerosis. *Arthritis Rheumatol* 2020;72(1):137–149. doi:10.1002/art.41058, PMID:31350829.
- [36] Park JH, Kwak BJ, Choi HJ, Kim OH, Hong HE, Lee SC, *et al*. PGC-1 α is down-regulated in a mouse model of obstructive cholestasis but not in a model of liver fibrosis. *FEBS Open Bio* 2021;11(1):61–74. doi:10.1002/2211-5463.12961, PMID:32860664.
- [37] De Bock K, Georgiadou M, Schoors S, Kuchnio A, Wong BW, Cantelmo AR, *et al*. Role of PFKFB3-driven glycolysis in vessel sprouting. *Cell* 2013;154(3):651–663. doi:10.1016/j.cell.2013.06.037, PMID:23911327.
- [38] Zhu Z, Liu Q, Sun J, Bao Z, Wang W. Silencing of PFKFB3 protects podocytes against high glucose-induced injury by inducing autophagy. *Mol Med Rep* 2021;24(5):765. doi:10.3892/mmr.2021.12405, PMID:34490476.
- [39] Sorrentino V, Menzies KJ, Auwerx J. Repairing Mitochondrial Dysfunction in Disease. *Annu Rev Pharmacol Toxicol* 2018;58:353–389. doi:10.1146/annurev-pharmtox-010716-104908, PMID:28961065.
- [40] Engelmann C, Clària J, Szabo G, Bosch J, Bernardi M. Pathophysiology of decompensated cirrhosis: Portal hypertension, circulatory dysfunction, inflammation, metabolism and mitochondrial dysfunction. *J Hepatol* 2021;75(Suppl 1):S49–S66. doi:10.1016/j.jhep.2021.01.002, PMID:34039492.